Available online at www.sciencedirect.com
SCIENCE DIRECT®
ELSEVIER
International Journal of Solids and Structures 42 (2005) 3075–3092
INTERNATIONAL JOURNAL OF SOLIDS and STRUCTURES
www.elsevier.com/locate/ijsolstr

An analytical molecular structural mechanics model for the mechanical properties of carbon nanotubes

J.R. Xiao [a,*], B.A. Gama [a], J.W. Gillespie Jr. [a,b,c]

[a] *Center for Composite Materials, University of Delaware, Newark, DE 19716, USA*
[b] *Department of Materials Science and Engineering, University of Delaware, Newark, DE 19716, USA*
[c] *Department of Civil and Structural Engineering, University of Delaware, Newark, DE 19716, USA*

Received 22 October 2004
Available online 10 December 2004

Abstract

An analytical molecular structural mechanics model for the prediction of mechanical properties of defect-free carbon nanotubes is developed by incorporating the modified Morse potential with an analytical molecular structural model. The developed model is capable of predicting Young's moduli, Poisson's ratios and stress–strain relationships of carbon nanotubes under tension and torsion loading conditions. Results on the mechanical properties of single-walled carbon nanotubes show that Young's moduli of carbon nanotubes are sensitive to the tube diameter and the helicity. Young's moduli of both armchair and zigzag carbon nanotubes increase monotonically and approach Young's modulus of graphite when the tube diameter is increased. The nonlinear stress–strain relationships for defect-free nanotubes have been predicted, which gives a good approximation on the ultimate strength and strain to failure of nanotubes. Armchair nanotubes exhibit higher tensile strength than zigzag nanotubes but their torsion strengths are identical based on the present study. The present theoretical investigation provides a very simple approach to predict the mechanical properties of carbon nanotubes.

Keywords: Nanotube; Molecular mechanics; Morse potential; Elastic properties; Stress–strain relationships; Strength

1. Introduction

The discovery of carbon nanotubes at the beginning of last decade (Iijima, 1991) has stimulated extensive research activities devoted entirely to nano-structures and their applications in materials science, chemistry,

* Corresponding author. Tel.: +1 30 283 18493; fax:+ 1 30 283 18525.
E-mail address: xiaoj@ccm.udel.edu (J.R. Xiao).

0020-7683/$ - see front matter © 2004 Elsevier Ltd. All rights reserved.
doi:10.1016/j.ijsolstr.2004.10.031

physics and engineering due to their exceptional physical properties: small size, low density, high stiffness, high strength and excellent electronic and thermal properties (Dresselhaus et al., 1996; Che et al., 2000; Nardelli et al., 2000; Yakobson and Avouris, 2001; Thostenson et al., 2001; Qian et al., 2002; etc.). Due to the high specific stiffness and strength, nanotubes represent a very promising material as reinforcements in composite materials.

Elastic properties of both multi- and single-walled nanotubes (SWNT) have been investigated extensively through experimentation (Treacy et al., 1996; Krishnan et al., 1998) and theoretical approaches (Yakobson et al., 1996; Wong et al., 1997; Yao and Lordi, 1998; Salvetat et al., 1999; Hernandez et al., 1999; Sanchez-Portal et al., 1999; Van Lier et al., 2000; Belytschko et al., 2002; etc.). SWNTs are remarkably stiff and strong. The tensile modulus and strength of nanotubes have been reported (Lourie and Wagner, 1998; Li et al., 2000) to range from 0.27 TPa to 3.6 TPa and 11 to 200 GPa, respectively. It is generally recognized that mechanical properties of nanotubes are dependent upon their structural details. For small single-walled nanotubes, although some results indicated that elastic properties are insensitive to the size of nanotubes (Lu, 1997; Jin and Yuan, 2002), quantum mechanics based computations have shown that Young's modulus increases with the tube diameter (Goze et al., 1999; Hernandez et al., 1999). Popov et al. (2000) derived some analytical expressions for the size-dependent elastic properties of single-walled nanotubes using Born's perturbation technique within a lattice-dynamics framework.

The theoretical approaches can be classified into two categories: namely the ''bottom up'' approach based on quantum/molecular mechanics including the classical molecular dynamics (MD) and *ab initio* methods, and the ''top down'' approach based on continuum mechanics. In general, *ab initio* methods give more accurate results than MD, but they are also much more computationally expensive (only suitable for small systems containing at most hundreds of atoms). As indicated by Qian et al. (2002), despite constant increases in available computational power and improvement in numerical algorithms, even classical molecular dynamics computations are still limited to simulating on the order of 10^6–10^8 atoms for a few nanoseconds. The simulation of larger systems or longer times must currently be left to continuum methods. However, at the nanoscale, theories for describing continuum materials have reached their limit. The accuracy of using these continuum theories becomes questionable in many of the most interesting cases of nanomechanics. Thus it would be very useful to have a nanomechanics theory that is seamless and generic to bridge the gap. Although several promising methods and approaches spanning multiple length scales have been developed towards achieving this goal (Tadmor et al., 1996; Abraham et al., 1998; Shenoy et al., 1999; Rudd and Broughton, 2000; Belytschko and Xiao, 2003; Xiao and Belytschko, 2004; Chung and Namburu, 2003; Qian et al., 2002), the link between atomistic and continuum descriptions of material properties is still not well established.

Some recent developments based on continuum mechanics have been reported for estimating elastic properties of nanotubes. Odegard et al. (2002) developed a continuum model to obtain a relation between effective bending rigidity and molecular properties of a graphene sheet by equating the molecular potential energy of nanotubes to the mechanical strain energy of a representative continuum truss model. Li and Chou (2003) developed a continuum mechanics model for mechanical properties of nanotubes successfully by linking the molecular mechanics constants of force fields and frame sectional stiffness parameters. Size-dependent Young's moduli and shear moduli of armchair and zigzag nanotubes have been predicted. Most recently, an analytical molecular mechanics model has been proposed by Chang and Gao (2003) to relate the elastic properties of a single-walled carbon nanotube to its atomic structure with calibrated force field constants. The developed approach is concise but capable of deriving closed form expressions for Young's modulus and Poisson's ratio as a function of the atomic structure of the nanotube. The force constants are determined by calibrating the model with experimental in-plane elastic constants of graphene sheet. Only tensile properties were studied by Chang and Gao (2003). However, all of the above-mentioned methods can only predict elastic constants like Young's moduli and/or Poisson's ratio of nanotubes because they were based on the force-field constants that imply that harmonic energy potential functions were used. In order to model the

mechanical behavior of nanotubes up to or beyond bond breaking, a more complex interatomic potential function has to be used. The Brenner potential function (Brenner, 1990) is considered more accurate and is more versatile, and it can handle changes in atom hybridization and bonds with atoms other than carbon. A continuum mechanics approach directly incorporating the Brenner potential function has been developed by Zhang et al. (2002) and Jiang et al. (2003) to model elastic properties and stress–strain relationships of carbon nanotubes based on a modified Cauchy–Born rule. The continuum strain energy density is obtained by averaging the energy stored in atomic bonds over bond orientations. Using the work-conjugate relationship between stress and strain, the stress and incremental modulus are derived from the strain energy density.

In this paper, we present a simple analytical molecular structural mechanics model incorporating the modified Morse potential function (Belytschko et al., 2002) to estimate elastic constants and stress–strain relationships of nanotubes under tensile and torsion loadings. The analytical model originated from Chang and Gao (2003) and was extended to model the torsion behavior of carbon nanotubes. By incorporating the modified Morse potential we are able to predict the mechanical properties not only Young's moduli and Poisson's ratio, but also the stress–strain relationships, hence, the strength and strain to failure of nanotubes. Detailed derivations are presented and the predicted results are demonstrated and discussed with a few computational examples. The present study shows that it is possible to develop analytical methodologies based on molecular mechanics to quantify mechanical behavior of a nanotube. The results are comparable to the corresponding published results from experiments, tight binding or molecular dynamics numerical calculations for armchair and zigzag carbon nanotubes.

2. Interatomic potential functions

There are several different potential functions available (Abell, 1985; Tersoff, 1988; Brenner, 1990) for describing C–C bond other than simple harmonic functions. Generally, the Tersoff–Brenner potential function is more accurate but it is complicated as presented in the atomistic-based analytical model by Jiang et al. (2003). Considering a single-walled carbon nanotube subjected to tension and torsion loadings, only bond stretching and angle variation terms are significant in the total system potential energy. The modified Morse potential function in Belytschko et al. (2002) is simple and is used in the present study. The modified Morse potential function was correlated to the Brenner potential function for strains below 10%. By using the simplified potential function in their molecular mechanics/dynamics models, Belytschko et al. (2002) studied the fracture behavior of nanotubes and excellent predictions have been achieved. The modified Morse potential function is given as follow:

$$E = E_{\text{stretch}} + E_{\text{angle}} \tag{1}$$

$$E_{\text{stretch}} = D_e\{[1 - \mathrm{e}^{-\beta(\Delta r)}]^2 - 1\} \tag{2}$$

$$E_{\text{angle}} = \frac{1}{2}k_\theta(\Delta\theta)^2[1 + k_{\text{sextic}}(\Delta\theta)^4] \tag{3}$$

where E_{stretch} is the bond energy due to bond stretch Δr, and E_{angle} is the bond energy due to bond angle variation $\Delta\theta$. The parameters calibrated by Belytschko et al. (2002) with the Brenner potential are as follows:

$$D_e = 0.6031\ \text{nN}\cdot\text{nm}, \quad \beta = 26.25\ \text{nm}^{-1} \tag{4}$$

$$k_\theta = 1.42\ \text{nN}\cdot\text{nm/rad}^2, \quad k_{\text{sextic}} = 0.754\ \text{rad}^{-4} \tag{5}$$

This set of parameters corresponds with the Brenner potential for strain below 10% and a separation (dissociation) energy of 124 kcal/mol (5.62 eV/atom).

As shown in the study by Belytschko et al. (2002), the force field shape of this simple potential function is essentially the same as that of the Brenner potential function before the inflection point (i.e. the maximum of the interatomic force) and totally different after the inflection point. The validation of using this simple interatomic potential function has been well studied by Belytschko et al. (2002) who reported that the fracture is essentially independent of the separation energy and depends primarily on the inflection point of the interatomic potential. Consequently, the shape of the potential function after the inflection point is not important to fracture behavior.

In this paper, a slightly modified value has been used for the constant k_θ which is taken from Chang and Gao (2003). As pointed out by Belytschko et al. (2002) the bond-angle-bending energy does not contribute to the stretch energy and has little effect on fracture. However, the bond-angle-bending potential plays an essential role in establishing an equilibrium configuration of the nanotube and it is associated with Young's modulus of the nanotube.

The stretch force and the angle-variation moment can be obtained from differentiations of Eqs. (2) and (3) as functions of bond stretch and bond angle variation, respectively:

$$F(\Delta r) = 2\beta D_e(1 - e^{-\beta\Delta r})e^{-\beta\Delta r} \tag{6}$$

$$M(\Delta\theta) = k_\theta\Delta\theta[1 + 3k_{\text{sextic}}(\Delta\theta)^4] \tag{7}$$

3. Molecular structural mechanics of nanotubes

A single-walled carbon nanotube can be viewed as a hollow cylinder rolled from a graphene sheet. The nanotube, composed of carbon hexagons, is usually indexed by a pair of integers (n_1, n_2) to represent its helicity. The diameter of the nanotube can be calculated as

$$D = \frac{\sqrt{3}a}{\pi}\sqrt{(n_1^2 + n_2^2 + n_1 n_2)} \tag{8}$$

where $a = 0.142$ nm is the C–C bond length.

Only two types of nanotubes: armchair ($n_1 = n_2$) and zigzag ($n_2 = 0$) nanotubes subjected to tensile and torsion loadings are studied in this paper.

3.1. Tensile response models

An armchair nanotube ($n_1 = n_2$) subjected to a longitudinal tensile stress is studied first. Fig. 1 shows an equilibrium configuration of the tube and the associated forces and moments in three chemical bonds a, b, b, and three bond angles α, β, β resulting from a bond elongation Δa and two bond angle variances $\Delta\alpha$ and $\Delta\beta$. The relationship between stress and the bond stretch and bond angle variation can be determined through equilibrium and geometry of the tube structure.

Similar to the idea of modeling the molecular structure as an effective "stick-spiral" system by Chang and Gao (2003), we use a stick with Eq. (6) to model the force-stretch relationship of the C–C bond and a spiral spring with Eq. (7) to model the angle bending moment resulting from an angular variation of bond angle. The stick is assumed to have an infinite bending stiffness.

Consider the force and moment acting on bond OA as shown in Fig. 1b. Force equilibrium to bond extension of stick OA leads to

$$f\sin\left(\frac{\alpha}{2}\right) = F(\Delta b) \tag{9}$$

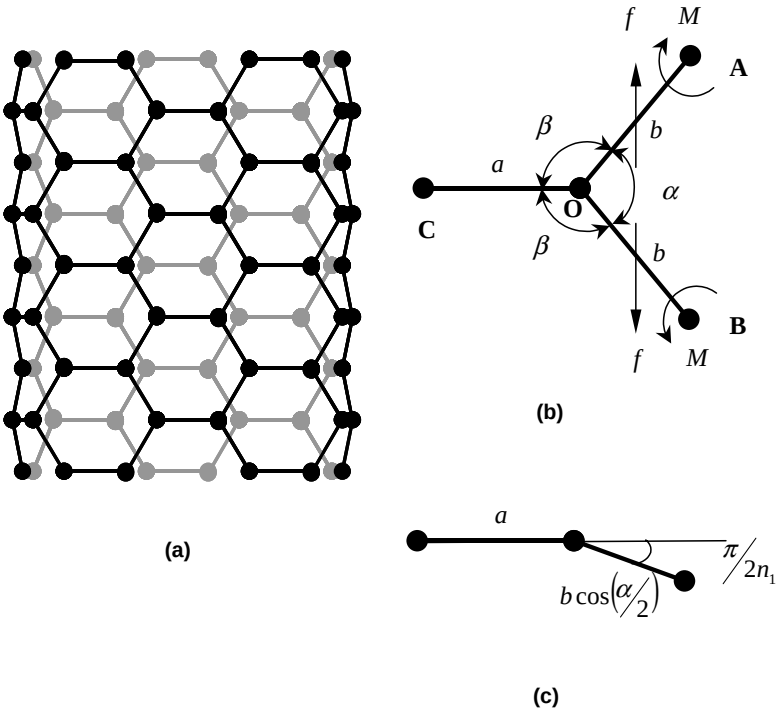

Fig. 1. Schematic illustration of (a) an armchair carbon nanotube, (b) analytical model for tension, and (c) geometry relationship.

The moment equilibrium to bond OA gives

$$f\frac{b}{2}\cos\left(\frac{\alpha}{2}\right) = M(\Delta\alpha) + M(\Delta\beta)\cos\varphi \tag{10}$$

where ϕ is the torsion angle between planes OA–OB and OA–OC, which is calculated as

$$\cos\varphi = -\frac{\tan\left(\frac{\alpha}{2}\right)}{\tan\beta} \tag{11}$$

For the armchair nanotube, the geometry relationships satisfy

$$\cos\beta = \cos\left(\pi - \frac{\pi}{2n_1}\right)\cos\left(\frac{\alpha}{2}\right) \tag{12}$$

where $\pi - \frac{\pi}{2n_1}$ is the angle of the bond OC to the plane OA–OB as shown in Fig. 1c.

Differentiating Eq. (12), one has

$$\Delta\beta = -\frac{\sin\left(\frac{\alpha}{2}\right)}{2\sin\beta}\cos\frac{\pi}{2n_1}\Delta\alpha \tag{13}$$

In the undeformed configuration, we take the relation $a = b$ though the calculation from Brenner potential function (Jiang et al., 2003) indicates that the bond length a and b are slightly different when the tube diameter changes.

The axial stress σ in the armchair nanotube can be defined as

$$\sigma = \frac{f}{tb\left(1+\cos\left(\frac{\alpha}{2}\right)\right)} \tag{14}$$

where t is the nanotube thickness and has been commonly assumed to be the interlayer spacing (0.34 nm) of graphite. The axial strain ε and circumferential strain ε' of armchair nanotube can be calculated as

$$\varepsilon = \frac{\Delta b \sin\left(\frac{\alpha}{2}\right) + \frac{b}{2}\cos\left(\frac{\alpha}{2}\right)\Delta\alpha}{b\sin\left(\frac{\alpha}{2}\right)} \tag{15}$$

$$\varepsilon' = \frac{\Delta b \cos\left(\frac{\alpha}{2}\right) - \frac{b}{2}\sin\left(\frac{\alpha}{2}\right)\Delta\alpha}{a + b\cos\left(\frac{\alpha}{2}\right)} \tag{16}$$

Then, Poisson's ratio can be defined as

$$v = -\frac{\varepsilon'}{\varepsilon} \tag{17}$$

The numerical procedure for stress–strain relationship is given as follows:

(1) For any given bond stretch Δb
(2) Determine f using Eqs. (9) and (6)
(3) Calculate stress at the current state using Eq. (14)
(4) Identify an equilibrium geometry with $\Delta\alpha$ and $\Delta\beta$ corresponding to Δb
  (a) Loop over angular variation $\Delta\alpha$
    (i) Obtain angular variation $\Delta\beta$ using Eq. (12)
    (ii) Calculate $M(\Delta\alpha)$ and $M(\Delta\beta)$ using Eq. (7)
    (iii) Exam the moment equilibrium equation (10)
  (b) End the angular variation loop
(5) Calculate strain at the current state using Eq. (15)

It should be noted that the angle α and β of armchair nanotubes have been found from *ab initio* calculations (Ye et al., 2001) where $\alpha \approx 2\pi/3$ and $\beta = \pi - \arccos[0.5\cos(\pi/2n_1)]$.

For a zigzag nanotube under tensile stress, the nomenclature and force and moment are shown in Fig. 2. The angle between planes OA–OB and OA–OC is given as

$$\cos\varphi = -\frac{\tan\left(\frac{\beta}{2}\right)}{\tan\alpha} \tag{18}$$

and the relationship between α and β leads to

$$\Delta\beta = \frac{2\cos\alpha}{\cos\frac{\beta}{2}}\cos\frac{\pi}{n_1}\Delta\alpha \tag{19}$$

With force equilibrium of stick OA, one has

$$f = \frac{F(\Delta a)}{\cos(\pi - \alpha)} \tag{20}$$

so the stress can be calculated as

$$\sigma = \frac{f}{ta\sin(\pi - \alpha)} \tag{21}$$

Considering the force equilibrium at point O, the stretch of stick OC can be related to the stretch of the stick OA by

$$F(\Delta b) = 2f \tag{22}$$

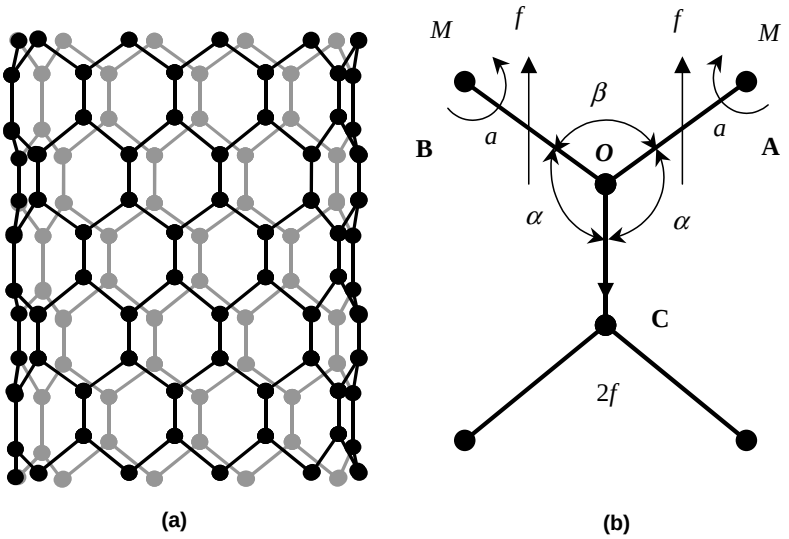

Fig. 2. Schematic illustration of (a) a zigzag carbon nanotube, and (b) analytical model for tension.

The moment equilibrium to bond OA leads to

$$f\frac{a}{2}\sin(\pi-\alpha)=M(\Delta\alpha)+M(\Delta\beta)\cos\varphi \tag{23}$$

The axial strain ε and circumferential strain ε' of the zigzag nanotube can be calculated as

$$\varepsilon=\frac{\Delta b+\Delta a\cos(\pi-\alpha)+a\sin(\pi-\alpha)\Delta\alpha}{b+a\cos(\pi-\alpha)} \tag{24}$$

$$\varepsilon'=\frac{\Delta a\sin(\pi-\alpha)-a\cos(\pi-\alpha)\Delta\alpha}{a\sin(\pi-\alpha)} \tag{25}$$

The stress–strain relationship for a zigzag tube is calculated in a similar manner to the armchair nanotube described above. For any bond stretch Δa, one can identify an unique equilibrium geometry with Δb, $\Delta\alpha$ and $\Delta\beta$ corresponding to Δa, such that the stress and strain can be calculated using Eqs. (21), (24) and (25). The approximate expressions of the angle α and β for zigzag nanotubes are taken as $\alpha\approx 2\pi/3$ and $\beta=\arccos[0.25-0.75\cos(\pi/n_1)]$ from *ab initio* calculation (Ye et al., 2001). It should be noted that when one takes $\alpha=\beta=2\pi/3$ and $n_1\to\infty$ the above procedures give the stress–strain relationship of the graphene sheet which is identical from both procedures.

3.2. Torsion response models

In this section, the shear behavior of nanotubes subjected to torsion loading is analyzed. Fig. 3 illustrates the forces and nomenclatures for analysis of armchair nanotube under the shear stress τ. The lengths of three bonds are a, b and c, respectively. The shear stress in two directions is same and can be defined as

$$\tau=\frac{f_1}{ta\sin\left(\frac{\alpha}{2}\right)} \tag{26}$$

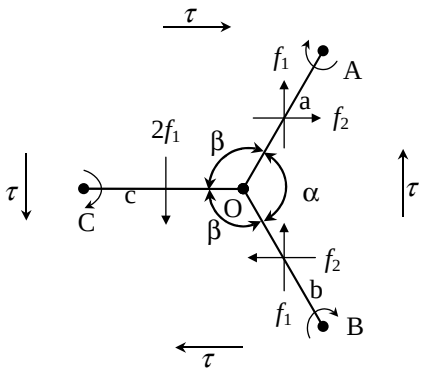

Fig. 3. Analytical model of an armchair carbon nanotube in shear.

$$\tau = \frac{f_2}{ta\left(1+\cos\left(\frac{\alpha}{2}\right)\right)} \tag{27}$$

Then, one has

$$f_2 \sin\left(\frac{\alpha}{2}\right) = f_1\left(1+\cos\left(\frac{\alpha}{2}\right)\right) \tag{28}$$

The force equilibrium on bond OA leads to

$$f_1 \sin\left(\frac{\alpha}{2}\right) + f_2 \cos\left(\frac{\alpha}{2}\right) = F(\Delta a) = -F(-\Delta b) \tag{29}$$

So the shear stress can be given as

$$\tau = \frac{F(\Delta a)}{ta\left(1+\cos\left(\frac{\alpha}{2}\right)\right)} \tag{30}$$

With the moment equilibrium on bond OA, one has

$$f_2 \frac{a}{2} \sin\left(\frac{\alpha}{2}\right) - f_1 \frac{a}{2} \cos\left(\frac{\alpha}{2}\right) = M(\Delta\beta)\cos\varphi \tag{31}$$

where $\cos\varphi$ is defined by Eq. (11). Substituting Eq. (28) into Eq. (31), one obtains

$$\frac{a}{2} f_1 = M(\Delta\beta)\cos\varphi \tag{32}$$

The shear strain of armchair nanotubes can be calculated as

$$\gamma = \frac{c\Delta\beta + \Delta b \sin\left(\frac{\alpha}{2}\right)}{a\left(1+\cos\left(\frac{\alpha}{2}\right)\right)} + \frac{(\Delta a + \Delta b)\cos\left(\frac{\alpha}{2}\right)}{2b\sin\left(\frac{\alpha}{2}\right)} \tag{33}$$

Then the shear modulus can be obtained as

$$G = \frac{\tau}{\gamma} \tag{34}$$

Again for any given bond stretch Δa, one can find an unique equilibrium configuration which satisfies all equations (26)–(34) described above, so that the shear stress–strain relationship is predicted analogous to the procedure for tensile behavior.

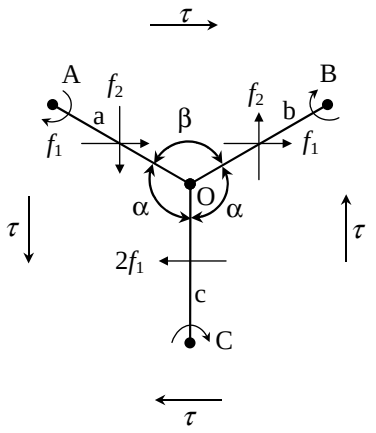

Fig. 4. Analytical model of a zigzag carbon nanotube in shear.

A zigzag nanotube under shear stress is depicted in Fig. 4. The associated variables can be defined as

$$f_1 = \tau bt \sin(\pi - \alpha) \tag{35}$$

$$\tau = \frac{F(\Delta a)}{ta(1 + \cos(\pi - \alpha))} \tag{36}$$

$$F(\Delta a) = -F(-\Delta b) \tag{37}$$

$$\frac{a}{2} f_1 = M(\Delta\alpha)\cos\varphi \tag{38}$$

and the shear strain γ of zigzag nanotube can be calculated as

$$\gamma = \frac{c\Delta\alpha + \Delta b \sin(\pi - \alpha)}{a(1 + \cos(\pi - \alpha))} + \frac{(\Delta a + \Delta b)\cos(\pi - \alpha)}{2b \sin(\pi - \alpha)} \tag{39}$$

Then, the shear stress–strain relationship for a zigzag tube under torsion loading is defined through Eqs. (35)–(39).

4. Results and discussions

4.1. Tensile behaviors

In this section, we present the predicted Young's modulus of nanotubes followed by their stress–strain relationships. It is known that there is a large variation of Young's moduli of nanotubes among published data from both experimental and theoretical studies. Krishnan et al. (1998) presented the experimental data as 1.3 $-0.4/+0.6$ TPa. Salvetat et al. (1999) measured Young's modulus of nanotubes as 0.816 ± 0.41 TPa. Variation from experimental results may be due to the presence of defects in nanotube specimens and inherent limitations of current experimental techniques. Different theoretical values can result from using different definitions of the effective thickness of nanotube, and by using different potential functions (force-constants) with different algorithms. For instance, Yakobson et al. (1996) used a thickness of 0.066 nm resulting in the graphite Young's modulus of 5.5 TPa. In order to avoid the confusion

on thickness definition, one can use in-plane stiffness as the product of the conventional Young's modulus with the tube thickness. As reviewed by Pantano et al. (2004) most quantum/molecular mechanics simulations resulted in similar graphite in-plane stiffness around 59 eV/atom = 360 J/m^2 though different effective thicknesses were assumed. It should be noted that the definition of effective thickness of nanotube does not affect in-plane properties in the present study. However, in order to compare the present results with recent progress (Belytschko et al., 2002; Jiang et al., 2003; Chang and Gao, 2003; Li and Chou, 2003) on nanotube mechanics, a thickness of 0.34 nm is used in the present study. Another interesting phenomena observed from theoretical investigations (such as the tight-binding results given by Goze et al. (1999), lattice-dynamical results given by Popov et al. (2000), atomistic-based continuum mechanics by Jiang et al. (2003), structural mechanics by Li and Chou (2003), and analytical molecular mechanics by Chang and Gao (2003)) is that Young's moduli are size-dependent at small tube diameters. Again due to the limitations of current experimental techniques it is hard to validate/extract such dependence experimentally.

Although there is discrepancy on Young's modulus of nanotubes it has been commonly recognized that nanotubes with large diameters have the same modulus as that of graphite and small diameter nanotubes exhibit some size-dependence. Experimental value for graphite (Blakslee et al., 1970) is about 1.06 TPa (corresponding to an in-plane stiffness of 360 J/m^2).

Available theoretical graphite values include 1.16 TPa (also size-independent nanotube value) by Belytschko et al. (2002) using molecular mechanics/dynamics with the modified Morse potential and 1.50 TPa by Overney et al. (1993) using MD with the Keating potential. Based on a lattice dynamics model with empirical force-constants, Lu (1997) calculated graphite (also nanotubes) Young's modulus to be about 0.972 TPa and Popov et al. (2000) gave results around 1.0 TPa for graphite. Li and Chou (2003) presented Young's modulus of carbon nanotube with larger diameters as 1.025 TPa using structural mechanics. Chang and Gao (2003) gave a graphite value of 1.06 TPa (360 J/m^2) using the same analytical structural model as the present investigation, but with force-constants (harmonic potential). The tight-binding methods also showed significant scatter in Young's modulus values with variations from 0.676 TPa (Molina et al., 1996) to 1.27 TPa (Goze et al., 1999). There are also many other predictions available in the literature.

Fig. 5 shows the calculated initial Young's modulus of nanotubes from the present models. The predicted Young's modulus of graphene sheet is 1.13 TPa (corresponding to an in-plane stiffness of 383 J/m^2), which agrees well with the experimental value and other theoretical values mentioned above. Differences between the experimental and theoretical graphite results may be due to the potential function and associated parameters. The simplified potential is correlated to the Brenner potential which is considered to be accurate. It should be noted that there are two different sets of parameters for carbon and hydrocarbons determined by Brenner through a best-fit of the potential to the binding energy of the C_2 diatomic molecule, and the binding energies and lattice constants of graphite, diamond, simple cubic, and face-centered-cubic (FCC) structures for pure carbon. Each set of parameters yielded different results and neither sets of parameters could fit C–C stretching force constants and bond lengths simultaneously. The parameters in the modified Morse potential corresponds to the second Brenner function that gives closer stretching force constants to experimental values but not identical (about 8% difference for double bonds). Approaches to select parameters that improve accuracy are beyond the scope of this research.

It is seen from Fig. 5 that the feature of the size-dependent Young's moduli is captured by the present simple model and Young's moduli for both armchair and zigzag nanotubes decrease with decreasing tube diameter and approach the predicted graphite value when the tube diameter is increased. For a given tube diameter, Young's modulus of armchair tubes is slightly larger than that of zigzag tubes. The maximum difference of armchair nanotube's moduli is less than 5% and could be considered size-independent. At small diameter (<2 nm), zigzag nanotubes exhibit a higher sensitivity of moduli to tube diameter as shown in Fig. 5 with a difference up to 19%. Some published data are also shown in Fig. 5 for comparison. The present model gives almost same trend as those of the tight-binding formulation by Goze et al. (1999) and continuum structural mechanics by Li and Chou (2003) although there exists difference at the plateau

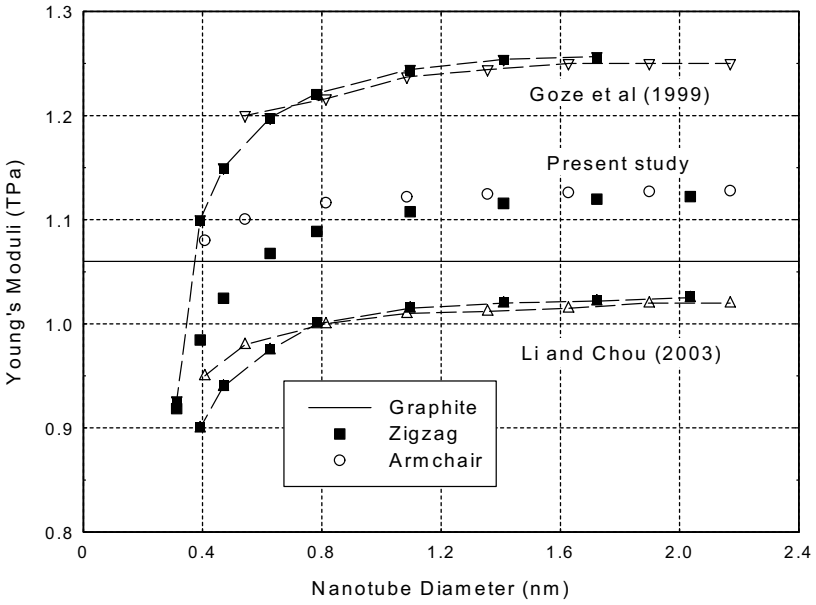

Fig. 5. Young's moduli of carbon nanotubes versus tube diameter.

level. It is interesting that when different values are normalized by their corresponding asymptotic value (i.e. predicted graphite value for large tube diameters), one obtains almost identical curves as shown in Fig. 6. In summary, the present values for single-walled nanotubes are in reasonable agreement with other theoretical and experimental values.

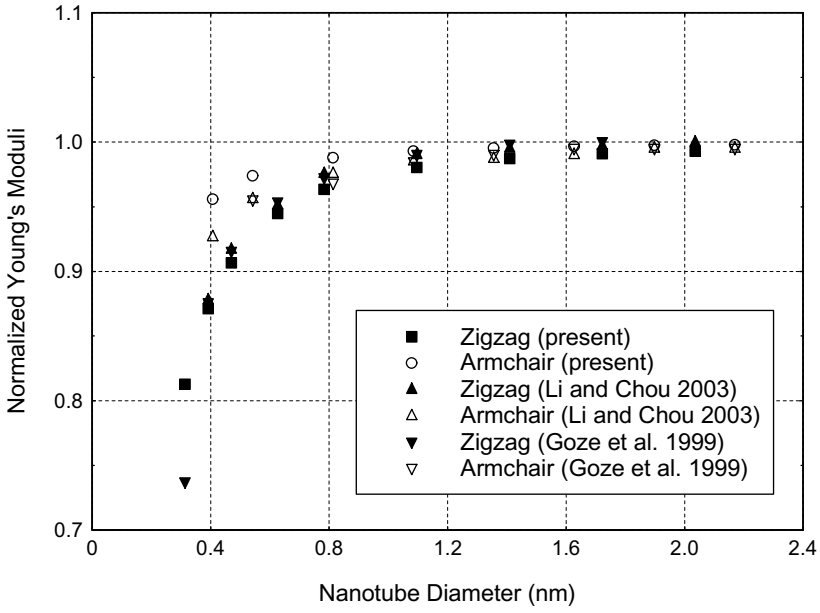

Fig. 6. Effect of tube diameter on normalized Young's moduli of carbon nanotubes.

It should be noted that all above-mentioned Young's moduli are the initial tangent modulus of carbon nanotubes. Secant moduli at different strains will be presented later in this section to illustrate the degree of nonlinearity in the stress–strain curve predicted prior to failure.

The dependence of Poisson's ratio to the tube diameter is shown in Fig. 7. The present predicted Poisson's ratio for both armchair and zigzag tubes decrease with increasing tube diameter, approaching the limit value of 0.20 for graphene sheet. It is seen that Poisson's ratio for zigzag tubes is more sensitive to the tube diameter than the armchair tubes. The results given by Popov et al. (2000) show the same trend as the present results for armchair tubes, but a different trend for zigzag tubes. It should be noted that the present prediction for large diameter nanotubes (>2 nm) and graphite is almost constant and in excellent agreement with the theoretical value (0.21) of Popov et al. (2000) based on a lattice-dynamics model. Although many investigations for Poisson's ratio of nanotubes have been conducted, there is no unique opinion that is widely accepted. The study by Lu (1997) showed that Poisson's ratio for single-walled nanotubes is almost a constant of 0.28. The tight-binding calculations (Goze et al., 1999) gave values of 0.247, 0.256 for (6, 6), (10, 10) armchair tubes and values of 0.275, 0.270 for (10, 0), (20, 0) zigzag tubes.

The stress–strain relationship of nanotubes is predicted using the above procedures up to the inflection point (i.e. the maximum of the interatomic force) only, though the procedure is able to give the post failure as the study by Jiang et al. (2003). However, the predicted post failure by the present model may not be reliable because the present model together with the simple interatomic potential function is not capable of describing the behaviors of the nanotube after the bonds are broken, such as formation of new bonds, rehybridization and structural transformations. From the experimental (Yu et al., 2000) and theoretical studies (Belytschko et al., 2002) on the tensile behaviors of nanotubes, it was found that the stress exhibits a sudden drop to zero when stress reaches the tensile strength and the fracture is brittle.

Fig. 8 shows the calculated stress–strain relationships for armchair and zigzag nanotubes. Only four different types of nanotubes (i.e. (4, 4), (12, 12) armchairs, and (4, 0), (20, 0) zigzags) are presented for illustration purpose. It should be noted that the present approach is developed based on the assumption of defect-free molecular structures so the predicted strengths are identical for the same type of helicity. The

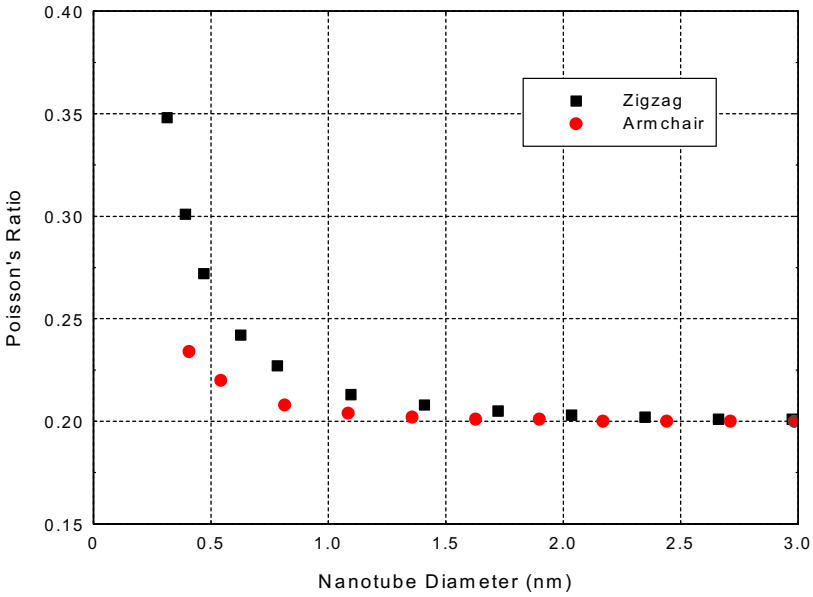

Fig. 7. Poisson's ratios of carbon nanotubes versus tube diameter.

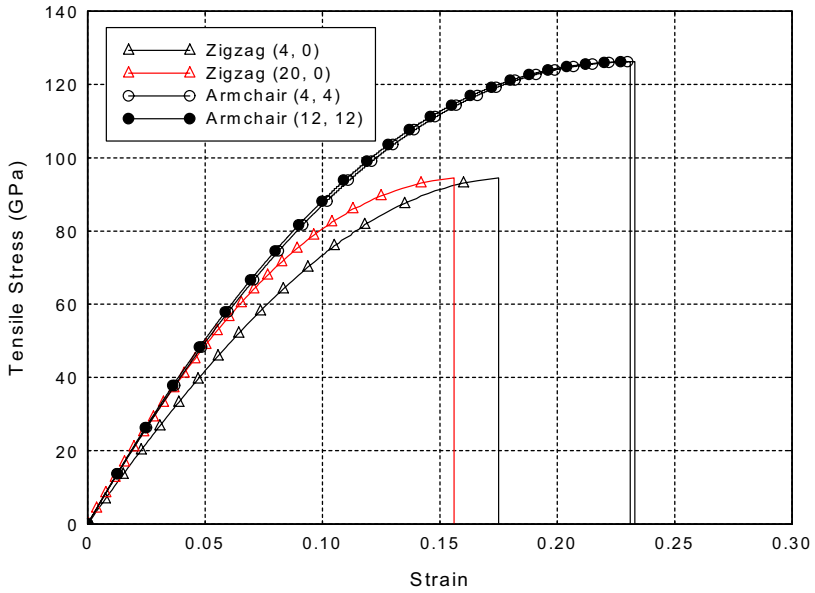

Fig. 8. Tensile stress–strain curves for armchair and zigzag nanotubes.

tensile behaviors of armchair nanotubes are almost identical with slightly different ultimate strains as the nanotube diameter changes because Young's moduli of this nanotube are less sensitive to their sizes as discussed above. Nevertheless, the tensile responses of zigzag nanotubes are much more sensitive to their diameter. As can be seen from Fig. 8, the predicted tensile strength (126.2 GPa) of armchair nanotubes is stronger than that (94.5 GPa) of zigzag nanotubes. The present predictions on strength of nanotubes show agreement with the calculated results from the molecular mechanics (Belytschko et al., 2002) where the tensile strength of 112 GPa and failure strain of 18.7% were predicted for (12, 12) armchair nanotube and 93.5 GPa and 15.2% for (20, 0) zigzag nanotube. The predicted failure strains in the present study are 23.1% for armchair nanotubes and 15.6–17.5% for zigzag nanotubes. Again these predictions agree well with the numerical results of Belytschko et al. (2002). The predicted nonlinear behaviors of nanotubes are also very similar to those modeled by using molecular mechanics (Belytschko et al., 2002). It should be noted that the predicted strengths and failure strains are significantly higher than the experimental values (11–63 GPa for strengths and 10–13% for failure strains) of Yu et al. (2000). This issue can be partially explained by the presence of defects. Another possible reason, as discussed by Belytschko et al. (2002), is that some slippage might occur at the attachments for the high-strain cases reported in Yu et al. (2000) resulting in a decrease in the measured values of Young's modulus and the failure strains. Because of the nonlinearity of stress–strain relationships, we also present the calculated secant modulus versus strain (up to 10%) for different nanotubes. In Fig. 9 it can be seen that the secant moduli decreases by 20–28% from the initial tangent moduli as the strain increases to 10% for each type of nanotubes.

4.2. Torsion response

The torsion response of nanotubes has received much less attention than the tensile behavior of nanotubes. There still exists difficulty in experimental techniques to measure either their modulus or strength. Theoretical studies have been conducted by Lu (1997), Popov et al. (2000) and Li and Chou (2003). The size-dependence of shear moduli was observed in all the above three references, though slightly different

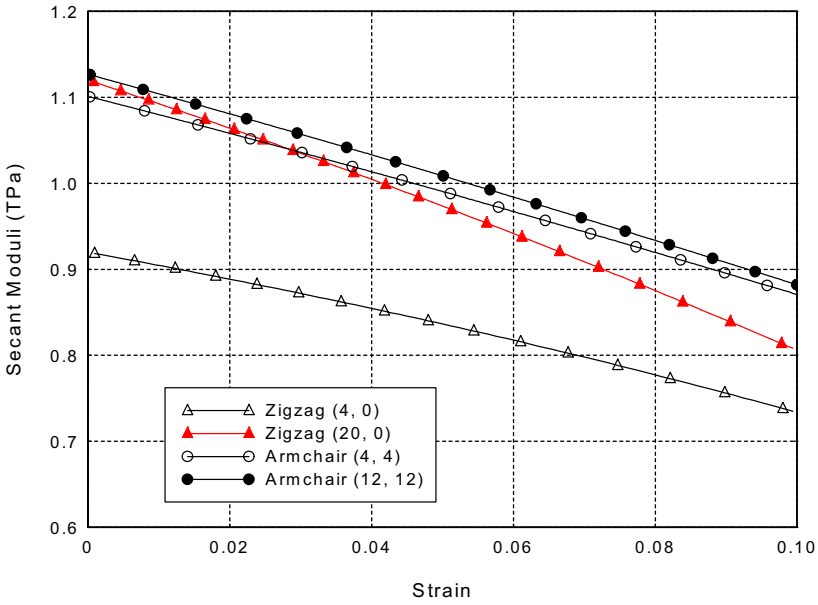

Fig. 9. Secant moduli of carbon nanotubes versus strain.

values for graphite and nanotubes with large diameters are predicted. The predicted graphite values for the shear modulus are 0.41 TPa by Popov et al. (2000), around 0.48 TPa by Lu (1997), and Li and Chou (2003). The shear modulus of the nanotube at small diameters is reduced from the graphite value by about 8% as predicted by Lu (1997) and 50% by Li and Chou (2003).

Fig. 10 shows the initial tangent shear moduli of nanotubes from the present study. It is seen that shear moduli for both armchair and zigzag nanotubes increase with increasing tube diameter and approach the predicted graphite value for larger diameter (>2 nm). The predicted graphite shear modulus of the present study is 0.47 TPa which shows good agreement with the experimental value (0.44 ± 0.3 TPa) of Blakslee et al. (1970), and is almost the same as other theoretical values reported by Lu (1997) and Li and Chou (2003). From the present study, it is shown that shear modulus of armchair and zigzag tubes possess similar size-dependent trends and similar finding has been reported by Li and Chou (2003) that the effect of tube chirality on the shear modulus is not significant based on their structural mechanics model. The size-effect on shear moduli from the present study is about 17% for small diameter nanotube compared with graphite value. Some published data are also included in Fig. 10 for comparison. Again there is discrepancy between experimental graphite result and theoretical values. Normalized shear moduli are presented in Fig. 11 to compare the size effect from different models. It can be seen that results by Li and Chou (2003) show higher size effect than the present study and results by Popov et al. (2000). The present study shows similar trends for zigzag tubes as that of Popov et al. (2000), but different in armchair tubes with which Popov et al. (2000) gave size-independent shear moduli. Jiang et al. (2003) also studied single-walled carbon nanotubes in pure torsion and presented relationships between the torque and the twist angle for several zigzag and armchair nanotubes. No specific value was reported for the shear modulus of nanotubes, but the normalized torque–twist curves indicated the shear moduli of armchair nanotubes are more sensitive to the tube diameter than zigzag nanotubes, and zigzag nanotubes possess higher resistance against torsion than armchair nanotubes.

Fig. 12 shows the calculated stress–strain relationships for armchair and zigzag nanotubes subjected to torsion loadings. Again, the four different types of nanotubes (i.e. (4, 4), (12, 12) armchairs, and (4, 0),

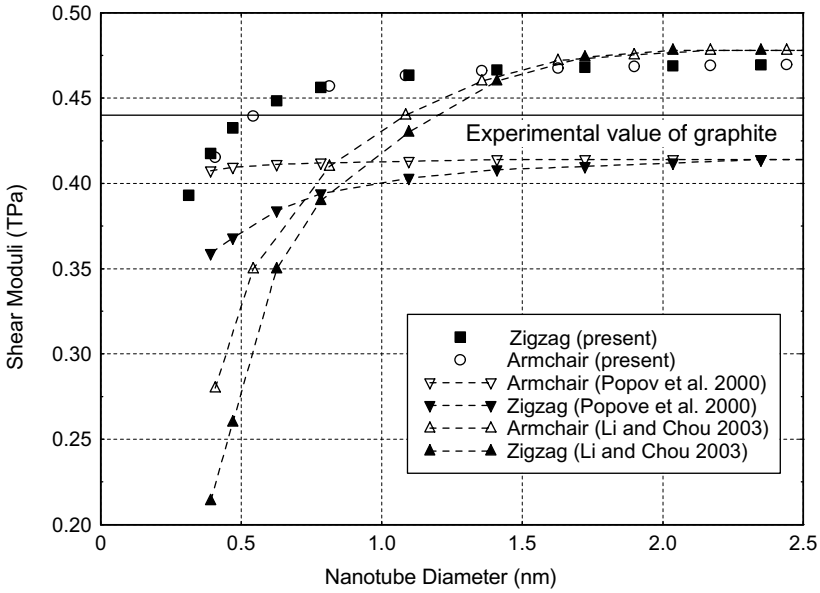

Fig. 10. Shear moduli of carbon nanotubes versus tube diameter.

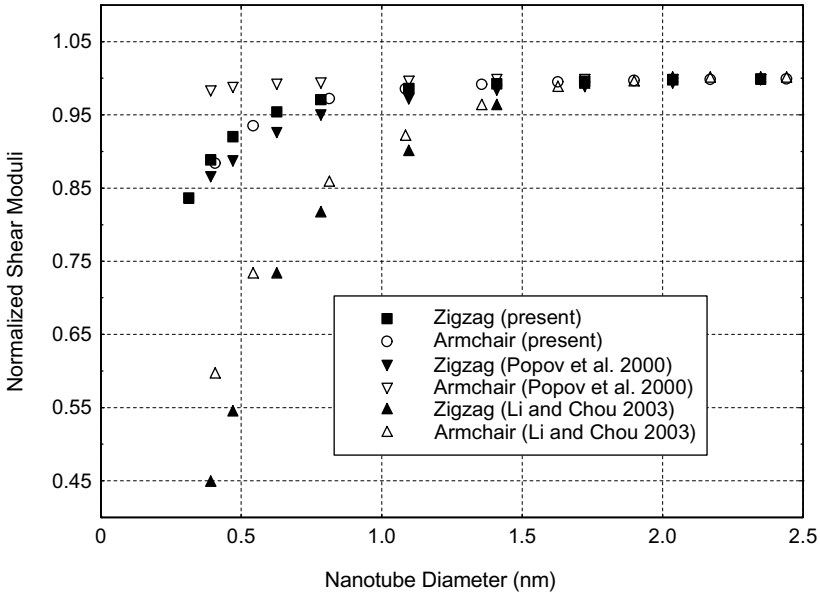

Fig. 11. Effect of tube diameter on normalized shear moduli of carbon nanotubes.

(20, 0) zigzags) are presented for illustration. The stress–strain relationships are calculated up to the inflection point as we did for tensile response though we do not know the failure modes when nanotubes are subjected to torsion loadings. Determination of such failure modes relies on experiments and quantum mechanics or MD simulations. Based on MD simulations with Brenner's many-body interatomic potential,

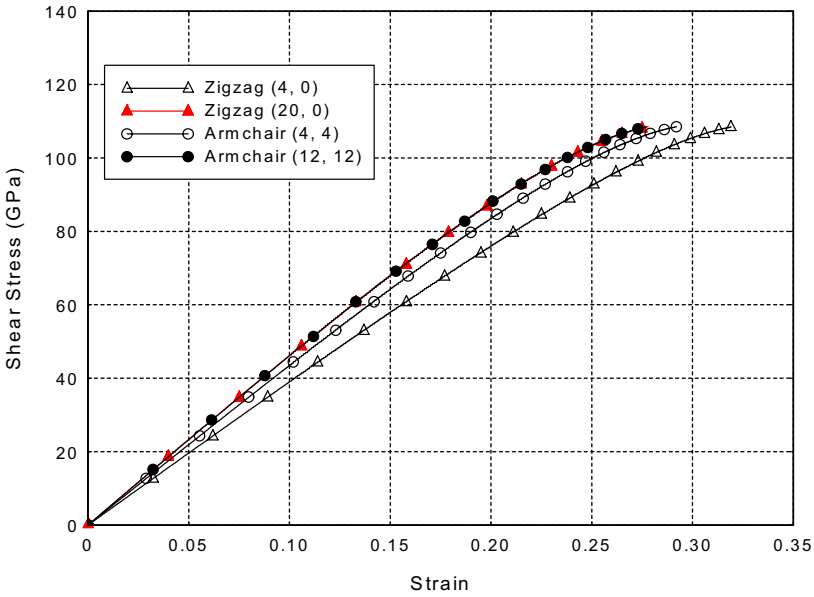

Fig. 12. Shear stress–strain curves for armchair and zigzag nanotubes.

Yakobson et al. (1996) indicated that nanotubes under torsion loading lead to a snap-through buckling without any bond breaking or switching. Unfortunately no specific value on critical buckling loading/strength was reported. The present study aims to give a reference value for this loading condition. We expect the predicted value should serve as the upper limit of the shear strength.

From Fig. 12, it can be seen that the present approach gives the same predicted strength for both types of nanotubes but with different failure strains. The predicted shear strength is 108 GPa. The stress–strain curves of (12, 12) armchair and (20, 0) zigzag nanotubes are identical because they have almost the same diameter. Smaller nanotube diameters give slightly higher failure strains, and the predicted failure strains range from 27% to 33%. It should be noted that the shear stress–strain relationships are almost linear up to the ultimate values for all examined nanotubes which implies the shear modulus for each tube is insensitive to strain from the present study.

5. Conclusions

By incorporating the modified Morse potential function into an analytical molecular structural mechanics model, the mechanical responses of armchair and zigzag nanotubes in tension and torsion conditions are investigated. The present approach is capable of predicting Young's moduli, Poisson's ratios, and stress–strain relationships of nanotubes. The analytical molecular mechanics model developed by Chang and Gao (2003) was extended to torsion loading condition. By incorporating the modified Morse potential into the developed model we have predicted the tensile and shear strengths and corresponding failure strains of single-walled carbon nanotubes. Young's moduli and Poisson ratios of nanotubes have been found to be sensitive to their sizes and chirality. Generally zigzag nanotubes exhibit higher sensitivity than armchair nanotubes when they are subjected to tensile loading. However, their shear moduli are insensitive to their chirality and show the same size-dependent trends for both armchair and zigzag nanotubes. The less dependence of shear modulus on chirality in the present study may be due to the absence of the torsional bond

interaction energy potential in the present simple model. The out-of-plane torsional bond interaction may become more dominant among the total system energy during the shear response comparing with the tensile response, particularly for small diameter nanotubes. Such effect is still under investigation. The tensile and torsion strengths have been studied by using the present methods and the same accuracy has been achieved compared to classical molecular mechanics/dynamics simulations. The armchair nanotubes possess higher tensile strength and failure strain than zigzag nanotubes. The shear performances of armchair and zigzag nanotubes are almost identical with slightly different failure strains. It should be noted that the present approach is much simpler than the classical molecular mechanics/dynamics model.

References

Abell, G.C., 1985. Empirical chemical pseudopotential theory of molecular and metallic bonding. Physical Review B 31, 6184–6196.

Abraham, F.F., Broughton, J.Q., Bernstein, N., Kaxiras, E., 1998. Spanning the continuum to quantum length scales in a dynamic simulation of brittle fracture. European Physical Letters 44 (6), 783–787.

Belytschko, T., Xiao, S.P., 2003. Coupling methods for continuum model with molecular model. International Journal for Multiscale Computational Engineering 1, 115–126.

Belytschko, T., Xiao, S.P., Schatz, G.C., Ruoff, R.S., 2002. Atomistic simulations of nanotube fracture. Physical Review B 65, 235–430.

Blakslee, O.L., Proctor, D.G., Seldin, E.J., Spence, G.B., Weng, T., 1970. Elastic constants of compression-annealed pyrolytic graphite. Journal of Applied Physics 41, 3373–3382.

Brenner, D.W., 1990. Empirical potential for hydrocarbons for use in simulating the chemical vapor-deposition of diamond films. Physical Review B 42, 9458–9471.

Chang, T., Gao, H., 2003. Size-dependent elastic properties of a single-walled carbon nanotube via a molecular mechanics modelnanotubes. Journal of the Mechanics and Physics of Solids 51, 1059–1074.

Che, J., Cagin, T., Goddard, W.A., 2000. Thermal conductivity of carbon nanotubes. Nanotechnology 11, 65–69.

Chung, P.W., Namburu, R.R., 2003. On a formulation for a multiscale atomistic-continuum homogenization method. International Journal of Solids and Structures 40, 2563–2588.

Dresselhaus, M.S., Dresselhaus, G., Eklund, P.C., 1996. Science of Fullerenes and Carbon Nanotubes. Academic Press, San Diego.

Goze, C., Vaccarini, L., Henrard, L., Bernier, P., Hernandez, E., Rubio, A., 1999. Elastic and mechanical properties of carbon nanotubes. Synthetic Metals 103, 2500–2501.

Hernandez, E., Goze, C., Bernier, P., Rubio, A., 1999. Elastic properties of single-wall nanotubes. Applied Physics A 68, 287–292.

Iijima, S., 1991. Helical microtubes of graphitic carbon. Nature 354, 56–58.

Jiang, H., Zhang, P., Liu, B., Huang, Y., Geubelle, P.H., Gao, H., Hwang, K.C., 2003. The effect of nanotube radius on the constitutive model for carbon nanotubes. Computational Material Science 28, 429–442.

Jin, Y., Yuan, F.G., 2002. Elastic properties of single-walled carbon nanotubes. AIAA-2002-1430.

Krishnan, A., Dujardin, E., Ebbesen, T.W., Yianilos, P.N., Treacy, M.M.J., 1998. Young's modulus of single-walled nanotubes. Physical Review B 58 (20), 14013–14019.

Li, C.Y., Chou, T.S., 2003. A structural mechanics approach for the analysis of carbon nanotubes. International Journal of Solids and Structures 40, 2487–2499.

Li, F., Cheng, B.S., Su, G., Dresselhaus, M.S., 2000. Tensile strength of single-walled carbon nanotubes directly measured from their microscopic ropes. Applied Physical Letters 77, 3161–3163.

Lourie, O., Wagner, H.D., 1998. Evaluation of Young's modulus of carbon nanotubes by micro-raman spectroscopy. Journal of Material Research 13, 2418–2422.

Lu, J.P., 1997. Elastic properties of carbon nanotubes and nanoropes. Physical Review Letters 79, 1297–1300.

Molina, J.M., Savinsky, S.S., Khokhriakov, N.V., 1996. A tight-binding model for calculations of structures and properties of graphitic nanotubes. Journal of Chemical Physics 104, 4652–4656.

Nardelli, M.B., Fattebert, J.L., Orlikowski, D., Roland, C., Zhao, Q., Bernholc, J., 2000. Mechanical properties, defects and electronic behavior of carbon nanotubes. Carbon 38, 1703–1711.

Odegard, G.M., Gates, T.S., Nicholson, L.M., Wise, K.E., 2002. Equivalent-continuum modeling with application to carbon nanotubes. NASA/TM-2002-211454.

Overney, G., Zhong, W., Tomanek, D., 1993. Structural rigidity and low-frequency vibrational modes of long carbon tubules. Zeitschrift für Physik D 27, 93–96.

Pantano, A., Parks, D.M., Boyce, M.C., 2004. Mechanics of deformation of single-and multi-wall carbon nanotubes. Journal of the Mechanics and Physics of Solids 52, 789–821.

Popov, V.N., Van Doren, V.E., Balkanski, M., 2000. Elastic properties of single-walled carbon nanotubes. Physical Review B 61, 3078–3084.

Qian, D., Wagner, G.J., Liu, W.K., Yu, M.F., Ruoff, R.S., 2002. Mechanics of carbon nanotubes. Applied Mechanics Review 55 (2), 495–533.

Rudd, R.E., Broughton, J.Q., 2000. Concurrent coupling of length scales in solid state systems. Physica Status Solidi B 217 (1), 251–291.

Salvetat, J.P., Bonard, J.M., Thomson, N.H., Kulik, A.J., Forro, L., Benoit, W., Zuppiroli, L., 1999. Mechanical properties of carbon nanotubes. Applied Physics A 69, 255–260.

Sanchez-Portal, D., Artacho, E., Soler, J.M., Rubio, A., Ordejon, P., 1999. Ab-initio structural, elastic, and vibrational properties of carbon nanotubes. Physical Review B 59, 12678.

Shenoy, V.B., Miller, R., Tadmor, E.B., Rodney, D., Phillips, R., Ortiz, M., 1999. An adaptive finite element approach to atomic-scale mechanics—the quasicontinuum method. Journal of the Mechanics and Physics of Solids 47 (3), 611–642.

Tadmor, E.B., Ortiz, M., Phillips, R., 1996. Quasicontinuum analysis of defects in solids. Philosophical Magazine A—Physics of Condensed Matter Structure Defects and Mechanical Properties 73, 1529–1563.

Tersoff, J., 1988. Empirical interatomic potential for carbon, with applications to amorphous-carbon. Physical Review Letters 61, 2872–2879.

Thostenson, E.T., Ren, Z., Chou, T.W., 2001. Advances in the science and technology of carbon nanotubes and their composites: a review. Composites Science and Technology 61, 1899–1912.

Treacy, M.M.J., Ebbesen, T.W., Gibson, J.M., 1996. Exceptionally high Young's modulus observed for individual carbon nanotubes. Nature 381, 678–680.

Van Lier, G., Van Alsenoy, C., Van Doren, V., Geerlings, P., 2000. *Ab initio* study of the elastic properties of single-walled carbon nanotubes and graphene. Chemical Physical Letters 326, 181.

Wong, E.W., Sheehan, P.E., Lieber, C.M., 1997. Nanobeam mechanics: elasticity, strength, and toughness of nanorods and nanotubes. Science 277, 1971–1975.

Yakobson, B.I., Avouris, P., 2001. Mechanical properties of carbon nanotubes. In: Dresselhaus, M.S., Dresselhaus, G., Avouris, P. (Eds.), Carbon Nanotubes, Topics in Applied Physics, vol. 80. Springer Verlag, Berlin/Heidelberg, pp. 287–329.

Yakobson, B.I., Brabec, C.J., Bernholc, J., 1996. Nanomechanics of carbon tubes: instability beyond linear response. Physical Review Letters 76, 2511–2514.

Yao, N., Lordi, V., 1998. Young's modulus of single-walled carbon nanotubes. Journal of Applied Physics 84, 1939–1943.

Ye, L.H., Liu, B.G., Wang, D.S., 2001. *Ab initio* molecular dynamics study on small carbon nanotubes. Chinese Physical Letters 18, 1496–1499.

Yu, M.F., Lourie, O., Dyer, M.J., Moloni, K., Kelly, T.F., Ruoff, R.S., 2000. Strength and breaking mechanism of multiwalled carbon nanotubes under tensile load. Science 287, 637–640.

Zhang, P., Huang, Y., Geubelle, P.H., Klein, P.A., Hwang, K.C., 2002. The elastic modulus of single-wall carbon nanotubes: a continuum analysis incorporating interatomic potentials. International Journal of Solids and Structures 39, 3893–3906.

Xiao, S.P., Belytschko, T., 2004. A bridging domain method for coupling continuum with molecular dynamics. Computer Methods in Applied Mechanics and Engineering 193, 1645–1669.